

Mohamed Abdelaty Habila<sup>1</sup>  
 Zeid Abdullah ALothman<sup>1</sup>  
 Rahmat Ali<sup>1</sup>  
 Ayman Abdel Ghafar<sup>1</sup>  
 Mohamed Slah El-Din Hassouna<sup>2</sup>

<sup>1</sup>Chemistry Department, College of Science, King Saud University, Riyadh, Kingdom of Saudi Arabia

<sup>2</sup>Department of Environmental Studies, Institute of Graduate Studies and Research, Alexandria University, Alexandria, Egypt

## Research Article

# Removal of Tartrazine Dye onto Mixed-Waste Activated Carbon: Kinetic and Thermodynamic Studies

Numerous studies have been performed on the conversion of individual types of waste into activated carbon (AC). However, this study focused on the evaluation of the simultaneous conversion of different types of wastes (palm, paper, and plastic wastes) into AC via copyrolysis. The tartrazine adsorption capacity onto the produced AC was optimized. The results showed that the carbon content of the AC improved as the calcium hydroxide concentration varied from 0.0 to 2.0 mol L<sup>-1</sup>. In addition, the volatile matter and ash content were reduced as the concentration of calcium hydroxide was increased from 0.0 to 2.0 mol L<sup>-1</sup>. The tartrazine adsorption capacity of the prepared AC samples increased as the calcium hydroxide concentration increased from 0.5 to 2 mol L<sup>-1</sup> at a carbonization temperature of 400°C for 2 h and a final activation temperature of 500°C for 1 h. Effective adsorption occurred at pH 2. The maximum adsorption capacity (74.9 mg g<sup>-1</sup>) was obtained with a contact time of 300 min and an initial tartrazine concentration of 150 ppm. The adsorption kinetics of tartrazine were modeled with pseudo-first order, pseudo-second order, and intraparticle diffusion models, which revealed that the tartrazine adsorption onto the AC showed a best fit with the pseudo-second order kinetic model. The thermodynamic parameters  $\Delta G^0$ ,  $\Delta H^0$ , and  $\Delta S^0$  indicated that the adsorption of tartrazine onto the AC was spontaneous and endothermic. The values of  $\Delta G^0$  were between -1.3 and -2.3 kJ mol<sup>-1</sup>, and the  $\Delta H^0$  and  $\Delta S^0$  values, in the temperature range of 25–50°C, were 9.12 kJ mol<sup>-1</sup> and 35.5 J mol<sup>-1</sup> K<sup>-1</sup>, respectively. In general, the thermodynamic parameters indicate that the adsorption is spontaneous and endothermic.

**Keywords:** Adsorption; Carbon content; Copyrolysis; Solid waste

*Received:* March 25, 2013; *revised:* August 25, 2013; *accepted:* September 18, 2013

**DOI:** 10.1002/clen.201300191

## 1 Introduction

The high production level and use of dyes worldwide generates colored wastewater, which is a cause of environmental concern. Textile companies, dye manufacturing industries, paper and pulp mills, tanneries, electroplating factories, distilleries, food companies, and a host of other industries discharge colored wastewater [1–4]. Currently, there are more than 10 000 dyes commercially available, and it is estimated that approximately 10–15% of the synthetic dyes that are used are washed away in waste streams during processing operations [5–8]. Tartrazine is a widely used yellow dye found in cosmetics, foodstuffs, medicines, and textiles. This dye is carcinogenic and causes allergic reactions [9]. Thus, the decolorization of this dye is an important process in wastewater treatment. Numerous studies have been performed on the decolorization of

wastewater [10–12], and adsorptive removal was found to be the most effective method [13, 14]. Activated carbon (AC) is commonly used for adsorptive removal. However, the use of commercially available AC is limited because of the high manufacturing costs [15]. Therefore, recent research has been focused on searching for economical and effective adsorbents for dye adsorption [16–19]. Agricultural waste like clay [20], durian shell [21], *Hevea brasiliensis* [22], banana stalk waste [23], termite feces [24], the marine red alga *Porphyra yezoensis* Ueda [25], chitosan [26], chitosan-coated bentonite beads [27], the forest waste *Xanthoceras sorbifolia* seed coat [28], and mango seed [29], are considered to be suitable alternative adsorbents. However, the use of agricultural waste products as adsorbents without a pretreatment process leads to an increase in the chemical oxygen demand and biological oxygen demand. In addition, the total organic carbon levels will increase because of the release of the soluble organic compounds that are included in the agricultural waste [30]. The conversion of these waste products into porous AC will circumvent these problems [31–35]. Santhi and Manonmani [36] reported that AC prepared from the peel of the *Cucumis sativa* fruit is effective in the decolorization of wastewater contaminated with malachite green dye. Chen et al. [37] reported the conversion of municipal sewage

**Correspondence:** M. A. Habila, Department of Chemistry, College of Science, Building # 5, PO Box 2455, King Saud University, Riyadh 11451, Kingdom of Saudi Arabia  
 E-mail: mhabila@ksu.edu.sa

**Abbreviations:** AC, activated carbon; FTIR, Fourier transform infrared

sludge into AC for the treatment of dye wastewater. Senthilkumar et al. [38] prepared AC from sisal fiber (*Agave sisalana* sp.) and pomegranate peel (*Punica granatum* sp.) for the effective removal of reactive orange 4 dye.

Domestic solid waste production in Saudi Arabia is 12 million tons per year; organic wastes represent the highest proportion of this waste (79%). Palm wastes are produced annually in Saudi Arabia at a rate of 100 000 tons per year [39]. By converting solid waste to AC, two positive environmental impacts are achieved. The unwanted wastes are reduced, and AC is produced as an alternative adsorbent that will overcome the problem of colored wastewater. The previous methods found in the literature typically pyrolyze one type of waste to produce AC; however, recently, a novel method for the recovery of wastes via their co-processing to produce liquid tar or gasification products has been proposed [40–42]. Therefore, we evaluated the simultaneous conversion of different types of waste (palm, paper, and plastic) into AC via copyrolysis. The effect of the final activation time at 500°C as well as the concentration of the activating agent (calcium hydroxide) was investigated. We aimed to optimize the copyrolysis temperature and time and thereby to maximize the carbon content of the produced AC. The efficiency of the prepared AC for tartrazine dye removal from aqueous solutions was evaluated. Batch adsorption experiments were conducted to evaluate the adsorption process over a wide range of operating conditions (sorbate concentration, pH, contact time, and adsorbent dose). In addition, the kinetics and thermodynamic parameters of the adsorption process were studied.

## 2 Materials and methods

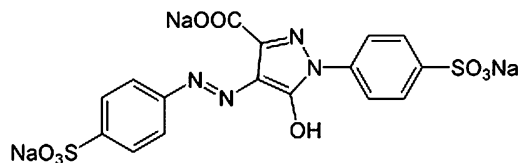
### 2.1 Materials

The precursors used in this study were palm waste, paper waste, and plastic waste that were collected from a municipal solid waste station in Riyadh. These types of waste are the most highly produced in Saudi Arabia. The elemental analysis of the precursor materials is shown in Tab. 1.

Tartrazine is a synthetic lemon yellow azo dye and its chemical structure is shown in Scheme 1. The preparation of the stalk solution is achieved by dissolving 1 g of tartrazine in 2 L of distilled water.

### 2.2 Preparation and characterization of the mixed-waste AC

In this study, a three-stage process [43] was modified for the preparation of mixed-waste AC. The mixed wastes (palm, paper, and plastic) were simultaneously copyrolyzed. The copyrolysis process was optimized to maximize the carbon content and the adsorption efficiency of the produced mixed-waste AC. In this process, the precursors are carbonized, impregnated, and then activated for a specific period of time. The pulverized palm stem, paper, and plastic waste were mixed with a ratio of 1:1:1 by weight and initially



**Scheme 1.** The chemical structure of tartrazine.

carbonized at 400°C for 2 h. The char that was produced was chemically activated with calcium hydroxide. The char (40 g) was mixed with 200 ml of a 2 mol L<sup>-1</sup> calcium hydroxide solution. The slurry was maintained in an ultrasonic bath at 40°C for 1 h to achieve maximum penetration of the solute molecules into the texture of the waste materials. The resulting homogenous slurry was dried at 110°C for 20 h, and the resulting impregnated char was activated at 500°C for 45 min. The obtained mixed-waste AC was allowed to cool and was washed with a 0.2 mol L<sup>-1</sup> HCl solution for 0.5 h to remove the surface ash. Subsequently, the sample was washed with distilled water numerous times to ensure the complete removal of the remaining acid (to reach a final pH of 6–7). After washing, the samples were dried at 110°C for 24 h, cooled in a desiccator, sieved through a 100-mesh filter (US Standard), retained on a 300-mesh filter, and stored in airtight bottles for further study. The carbon yield of each sample was calculated using the following Eq. (1):

$$\text{Yield (\%)} = \left( \frac{W_1}{W_0} \right) \times 100 \quad (1)$$

where  $W_1$  is the dry weight (g) of the final mixed-waste AC and  $W_0$  is the dry weight (g) of the precursor material.

The samples were examined using a Jeol (JSM-6380 LA) scanning electron microscope (Japan). The Fourier transform IR (FTIR) spectra of the samples were recorded using a spectrophotometer (Thermo Scientific, USA). Elemental analysis was performed using a Perkin Elmer Series II CHN analyzer.

### 2.3 Batch adsorption studies

The prepared mixed-waste AC (0.03 g in each flask) was transferred to 100 ml Erlenmeyer flasks and 80 ml of tartrazine solution (50 ppm) were added. The mixture was placed on a shaker at 150 rpm for 5 h at 25°C. The solution was filtered, and the tartrazine concentrations were determined by spectrometry at the wavelength of maximum absorbance, 400 nm, using a double beam UV-Vis spectrophotometer (Thermo Scientific). The blank replicates were prepared without adding AC. The same procedures were followed to evaluate the effect of temperature on the adsorption capacity.

The adsorption capacity of the AC samples was evaluated using the following Eq. (2):

$$Q_e = \frac{(C_0 - C_e)V}{M} \quad (2)$$

where  $Q_e$  is the adsorption capacity (mg g<sup>-1</sup>),  $C_0$  is the initial concentration of the tartrazine,  $C_e$  is the equilibrium concentration of the tartrazine,  $V$  is the volume of the solution (L), and  $M$  is the mass of the adsorbent (g).

**Table 1.** The elemental analysis of the precursor materials

Element	Palm stems	Waste paper	Plastic
Carbon (%)	45.56	37.83	91.42
Hydrogen (%)	5.91	5.57	7.82
Nitrogen (%)	0.82	0.08	0.12

### 3 Results and discussion

#### 3.1 The yield and properties of the prepared mixed-waste AC

The overall yield of AC increased as the calcium hydroxide concentration increased from 0.0 to 2 mol L<sup>-1</sup>. The higher yield of mixed-waste AC may be due to the inhibition of the formation of volatile matter by the activating agent (calcium hydroxide). The inhibiting effect of chemical activation on the volatile matter increases with a higher concentration, thereby increasing the carbon yield, enhancing the aromatic condensation reactions and facilitating the evolution of molecular hydrogen from the hydroaromatic structure of the precursor. The liberation of the hydrogen makes available some active sites on adjacent molecules that can undergo aromatization (polymerization) reactions. As a result of these reactions, the volatile molecules are stabilized, and the carbon yield is increased.

The FTIR spectra of the AC prepared from the mixed waste showed the following bands: 3650 and 3629 cm<sup>-1</sup>, which are related to the OH stretching vibration; 3440 and 3428 cm<sup>-1</sup>, arising from the NH stretching vibration in primary amines; 2928 cm<sup>-1</sup> and approximately 3100 cm<sup>-1</sup>, which are related to the aliphatic and aromatic CH stretching vibration; and 1700 cm<sup>-1</sup>, which is related to the CO stretching vibration. In addition, bands were detected at approximately 1600, 1585, and 1514–1450 cm<sup>-1</sup>, which are related to CC stretching in an aromatic ring.

Table 2 shows the ultimate and proximate analysis of the AC samples that were obtained from the copyrolysis of the mixed waste and activated with different concentrations of calcium hydroxide. The results showed a reduction in the volatile matter and ash content as the concentration (impregnation ratio) of calcium hydroxide was increased from 0 to 2 M. This reduction may have been caused by the inhibition of excessive burn-off as the concentration of calcium hydroxide increased, resulting in a higher yield of carbon and fixed carbon and a lower content of volatile matter and ash. The same trend was observed by increasing the activation time at 500°C. In addition, the carbon content (fixed carbon and elemental carbon) increased as the calcium hydroxide concentration increased. The value of elemental carbon was consistent with that of fixed carbon, and, for each sample, the fixed carbon value was lower than that of the elemental carbon.

#### 3.2 The effect of chemical and physical activation on the adsorption capacity (mg g<sup>-1</sup>)

The tartrazine adsorption capacity of the prepared AC samples increased as the calcium hydroxide concentration increased from 0.5

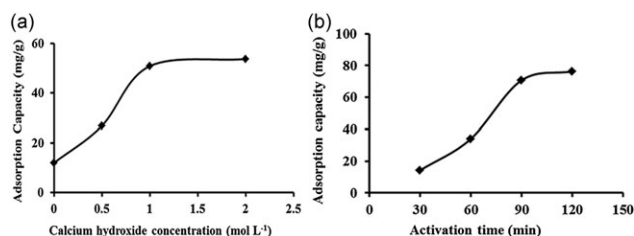


**Figure 1.** The effect of calcium hydroxide concentration (a) and final activation time at 500°C (b) on the tartrazine adsorption capacity (mg g<sup>-1</sup>) of mixed-waste AC prepared by copyrolysis of mixed waste.

to 2 mol L<sup>-1</sup> with carbonization at 400°C for 2 h and final activation at 500°C for 1 h (Fig. 1a). The same trend was observed when we increased the final activation time at 500°C from 30 to 120 min (Fig. 1b). These results were correlated with the properties of the AC, as shown in Tab. 2. The increase in the adsorption capacity for tartrazine removal with increasing calcium hydroxide concentration and increasing activation time at 500°C occurs because the chemical and physical activation promotes porosity in the carbon. A higher level of carbon porosity provides increased access to the bulky molecules of tartrazine, thereby raising its removal efficiency [44]. The scanning electron microscopy images (Figs. 2 and 3) showed the micro-porosity of the mixed-waste AC that was produced from the mixed waste and confirmed that chemical activation and physical activation with calcium hydroxide widen the pores and promote porosity in carbon, explaining the improvement in the adsorption capacity. Therefore, AC can be prepared by simultaneous copyrolysis of mixed solid waste and is effective for dye removal.

### 3.3 Adsorption studies

#### 3.3.1 The effect of pH

The pH of the aqueous solution is an important factor in controlling the surface charge of the adsorbent and the degree of ionization or polarity of the adsorbate in the solution [45]. Therefore, the role of the hydrogen ion concentration was examined using solutions with pH values ranging from 2 to 14. Figure 4 shows that the maximum adsorption capacity of the mixed waste AC for the tartrazine dye was obtained at a pH of 2 and was 72.03 mg g<sup>-1</sup>. The adsorption capacity decreased to 24.24 mg g<sup>-1</sup> at pH 5, and a subsequent increase in the pH caused the adsorption capacity to increase again until it reached 50.95 mg g<sup>-1</sup> at pH 10. This result may be attributed to the presence of various functional groups, such as OH, NH<sub>2</sub>, CC, and CO,

**Table 2.** Proximate and ultimate analysis of carbon samples obtained through copyrolysis of mixed waste

Activation condition		Proximate analysis (wt%, dry)				Ultimate analysis (wt%, dry basis)			
Calcium hydroxide (mol L <sup>-1</sup> )	Activation time (min)	Moisture	Volatile matter	Ash	Fixed carbon	Carbon	Hydrogen	Nitrogen	Oxygen
0	60	2.354	26.667	5.912	65.067	67.56	2.84	1.23	28.37
0.5	60	2.742	24.443	10.487	62.328	71.88	5.14	0.86	22.12
1	60	2.807	21.761	10.828	64.604	72.05	4.54	1.05	22.36
2	60	2.874	17.556	9.664	69.906	75.34	3.22	0.84	20.60
1	30	3.191	23.443	7.692	65.674	70.59	3.31	1.02	25.08
1	60	3.328	21.997	8.211	66.464	73.68	6.33	0.45	19.54
1	90	3.481	18.766	8.836	68.907	74.03	3.14	1.14	21.69
1	120	3.846	15.33	11.158	69.666	74.85	2.77	1.12	21.26

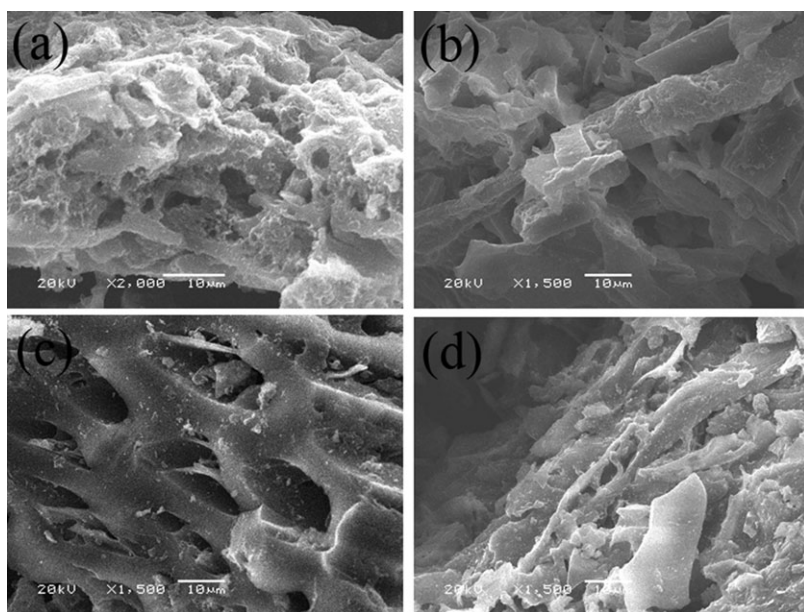


**Figure 2.** Scanning electron microscope image of mixed-waste AC prepared from coprolysis of mixed wastes with a carbonization temperature of 400°C for 2 h, chemical activation with (a) 0.0 mol L<sup>-1</sup>, (b) 0.5 mol L<sup>-1</sup>, (c) 1.5 mol L<sup>-1</sup>, and (d) 2 mol L<sup>-1</sup> calcium hydroxide and a final activation temperature of 500°C for 1 h.

as indicated from the FTIR results, and also to the presence of partially charged groups in the tartrazine structure, such as COO, SO<sub>3</sub>, and OH. The presence of these groups allows the formation of covalent bonds, columbic forces, hydrogen bonds, or weak van der Waals forces. The occurrence of the double bond serves to enhance the interaction between the dye and the AC [46].

### 3.3.2 The effect of contact time and initial tartrazine concentration

The amount of tartrazine adsorbed onto the mixed-waste AC was studied as a function of the contact time at different initial concentrations at 30°C and at the desired pH. Figure 5 shows the

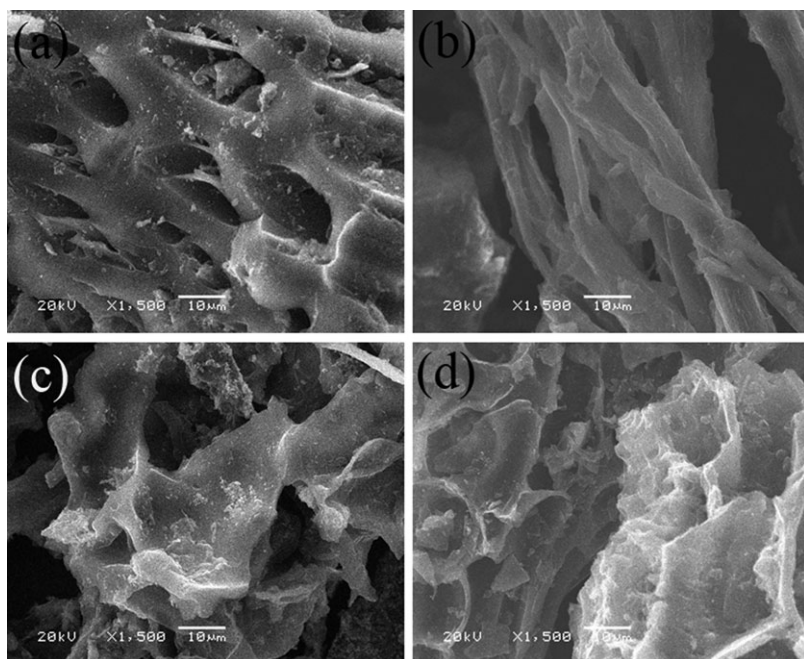


**Figure 3.** Scanning electron microscope image of mixed-waste AC prepared from coprolysis of mixed wastes with a carbonization temperature of 400°C for 2 h, chemical activation with 0.5 mol L<sup>-1</sup> calcium hydroxide and a final activation temperature of 500°C for (a) 0.5, (b) 1.0, (c) 1.5, and (d) 2 h.



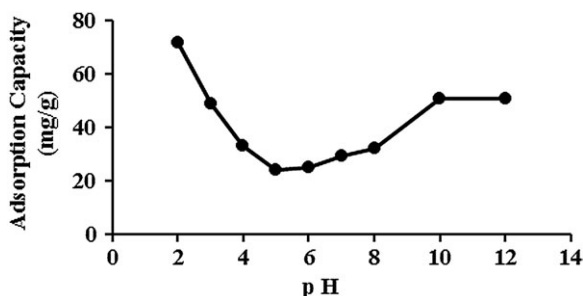


Figure 4. The effect of pH on tartrazine adsorption onto mixed-waste AC.

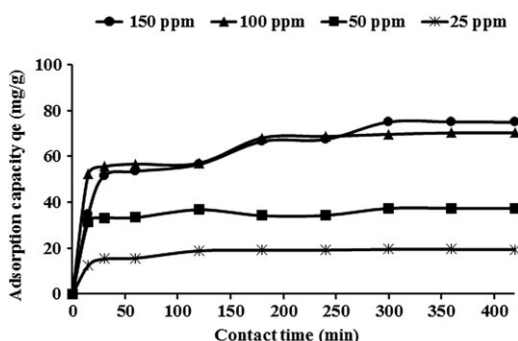


Figure 5. The effect of contact time and initial tartrazine concentration on tartrazine adsorption onto mixed-waste AC.

effect of contact time on tartrazine adsorption by mixed-waste AC for four different concentrations of tartrazine (25, 50, 100, and 150 ppm). The amount of tartrazine that was adsorbed increased with increasing contact time. The adsorption rate was rapid at the beginning of the adsorption process, and then the rate decreased and became constant after the equilibrium point. The saturation point is nearly reached at 300 min, and at this time the tartrazine that is desorbing from the mixed-waste AC is in a state of dynamic equilibrium with that being adsorbed onto the mixed-waste AC. The amount of tartrazine adsorbed at the equilibrium time reveals the maximum adsorption capacity of the mixed-waste AC. The removal of tartrazine increased from 19 to 74.9 mg g<sup>-1</sup> as the initial concentration increased from 25 to 150 ppm, indicating that the removal is affected by the initial concentration. The mass transfer driving force increased when the initial concentration increased and, therefore, resulted in a higher adsorption capacity. At low concentrations, the ratio of the available surface of the mixed-waste AC to the initial

tartrazine concentration is larger, and the removal becomes independent of the initial concentration, whereas at high tartrazine concentrations, this ratio is low. Therefore, we concluded that the initial concentration significantly affects the adsorption capacity.

### 3.3.3 Kinetic studies

Studies of the adsorption rate are important for the design of batch adsorption systems. The modeling of kinetics data aids in the selection of the optimum operating conditions. Lagergren's pseudo-first order equation [47] is expressed as follows:

$$\frac{dq_t}{dt} = k_1(q_e - q_t) \quad (3)$$

where  $q_e$  and  $q_t$  are the adsorption capacities at equilibrium and at time  $t$ , respectively, and  $k_1$  is the rate constant of the pseudo-first order adsorption (min<sup>-1</sup>). After integrating and applying boundary conditions,  $q_t = 0$  to  $q_t = q_t$  at  $t = 0$  to  $t = t$ , the integrated form of Eq. (3) becomes the following:

$$\log(q_e - q_t) = \frac{\log q_e - (k_1 t)}{2.303} \quad (4)$$

The pseudo-first order rate constant,  $k_1$ , is calculated by plotting the graph of  $\log(q_e - q_t)$  versus time  $t$  (Fig. 6a). The calculated  $k_1$  values and the corresponding linear regression correlation coefficient values are shown in Tab. 3. The linear regression correlation coefficient value,  $R^2$ , was low and the calculated  $q_e$  values (14.8, 8.11, 35.7, and 35.4 mg g<sup>-1</sup>) are significantly different from the experimental  $q_e$  values (19, 37.32, 69.59, and 74.96 mg g<sup>-1</sup>) for initial tartrazine dye concentrations of 25, 50, 100, and 150, respectively, indicating that this model cannot be applied to predict the adsorption kinetics.

The pseudo-second order kinetic rate equation is expressed as follows [48]:

$$\frac{dq_t}{dt} = k_2(q_e - q_t)^2 \quad (5)$$

where  $q_e$  and  $q_t$  are the adsorption capacities at equilibrium and at time  $t$ , respectively, and  $k_2$  is the rate constant of the pseudo-second order adsorption (g mg<sup>-1</sup> min<sup>-1</sup>). After integrating and applying boundary conditions,  $q_t = 0$  to  $q_t = q_t$  at  $t = 0$  to  $t = t$ , the integrated form of Eq. (5) becomes the following:

$$\frac{t}{q_t} = \frac{1}{k_2 q_e^2} + \frac{1}{q_e} t \quad (6)$$

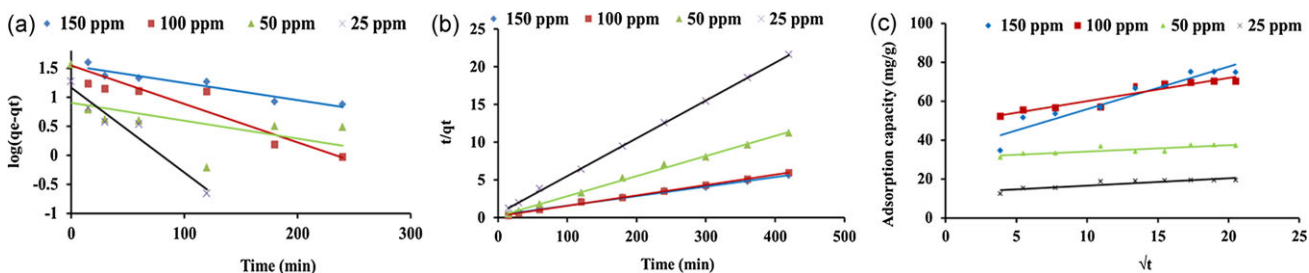


Figure 6. Plots of Lagergren's pseudo-first order (a), pseudo-second order (b), and intraparticle diffusion models (c) for tartrazine adsorption onto mixed-waste AC.

**Table 3.** The parameters of the kinetic constants obtained for tartrazine adsorption onto mixed-waste AC

Pseudo-first order					Pseudo-second order					Intraparticle diffusion model		
$C_i$ (ppm)	$q_{e,exp}$ (mg g <sup>-1</sup> )	$k_1$ (10 <sup>-3</sup> ) (min <sup>-1</sup> )	$q_{e,cal}$ (mg g <sup>-1</sup> )	$R^2$	$k_2$ (10 <sup>-4</sup> ) (g mg <sup>-1</sup> min <sup>-1</sup> )	$q_{e,cal}$ (mg g <sup>-1</sup> )	$h$ (mg g <sup>-1</sup> min <sup>-1</sup> )	$R^2$		$k_{id}$ (mg g <sup>-1</sup> min <sup>-1</sup> )	$C$ (mg g <sup>-1</sup> )	$R^2$
25	19	0.033	14.8	0.94	$4.7 \times 10^{-3}$	19.9	1.86	0.999		0.384	12.723	0.80
50	37.32	0.007	8.11	0.28	$3.4 \times 10^{-3}$	37.5	4.78	0.997		0.325	30.828	0.73
100	69.59	0.015	35.7	0.87	$9.6 \times 10^{-4}$	72.4	5.03	0.997		1.193	48.042	0.90
150	74.96	0.0069	35.4	0.90	$4.3 \times 10^{-4}$	79.3	2.7	0.993		2.186	34.005	0.91

where  $t$  is the contact time (min), and  $q_e$  (mg g<sup>-1</sup>) and  $q_e^2$  (mg g<sup>-1</sup>) are the amount of solute that is adsorbed at equilibrium. Figure 6b shows the linear relationship of the plot of  $t/q_t$  versus  $t$ , from which  $q_e$  and  $k$  can be determined from the slope and intercept, respectively.

The calculated  $k_2$  values and the corresponding linear regression correlation coefficient values are shown in Tab. 3. The results showed that the calculated  $q_e$  values (19.9, 37.5, 72.4, and 79.3 mg g<sup>-1</sup>) are in agreement with the experimental  $q_e$  values (19, 37.32, 69.59, and 74.96 mg g<sup>-1</sup>) for initial tartrazine dye concentrations of 25, 50, 100, and 150 ppm, respectively.

The intraparticle diffusion model was tested to identify the diffusion mechanism [49] and is expressed as follows:

$$q_t = k_{id}t^{1/2} + C \quad (7)$$

where  $k_{id}$  is the intraparticle diffusion rate constant (mg g<sup>-1</sup> min<sup>-1/2</sup>), and  $C$  is the intercept (mg g<sup>-1</sup>).

The plot of  $q_t$  versus  $t^{1/2}$  gave a straight line, and the values of  $k_{id}$  were determined from the slopes of the plots. The values of  $C$  provided information about the boundary layer, i.e., a larger value for the intercept indicated that there was a larger contribution of the adsorption at the surface. The data for tartrazine adsorption onto the mixed-waste AC that were applied to the intraparticle diffusion model are shown in Fig. 6c, and the results are shown in Tab. 3. The results showed that at low tartrazine concentrations of 25 and 50 ppm, the value of  $R^2$  was 0.80 and 0.73, respectively, whereas at higher tartrazine concentrations of 100 and 150 ppm the value of  $R^2$  was 0.90 and 0.91, respectively. These results indicate that the adsorption of tartrazine molecules onto the mixed-waste AC is a diffusion-controlled process only at a high concentration.

Table 3 shows that among these three models, the pseudo-second order kinetic equation had high  $R^2$  values, and the experimental  $q_e$  values are in agreement with the calculated  $q_e$  values. The low values of  $R^2$  for the pseudo-first order model indicated that this model did not fit the data well. Therefore, we concluded that the pseudo-second order kinetic model provided the best description of the mechanism of adsorption of tartrazine onto the prepared mixed-waste AC.

### 3.3.4 The effect of the adsorbent dose

The effect of the mixed-waste AC dose on the tartrazine adsorption process was evaluated. The adsorption capacity decreased from 68.9 to 7.7 mg g<sup>-1</sup> with an increase in the adsorbent concentration from 0.3 to 6 g L<sup>-1</sup>, with an initial tartrazine concentration of 150.9 ppm (Fig. 7). This result shows that at a low mixed-waste AC dose, all of the carbon surfaces are in contact with the tartrazine, allowing the maximum interaction.

### 3.3.5 Thermodynamic study

The thermodynamic parameters, free energy ( $\Delta G^0$ ), enthalpy ( $\Delta H^0$ ), and entropy ( $\Delta S^0$ ), were evaluated using the following equations:

$$\log K_d = \frac{\Delta S^0}{2.303R} - \frac{\Delta H^0}{2.303RT} \quad (8)$$

$$\Delta G^0 = -RT \ln K_d \quad (9)$$

where  $K_d$  is the equilibrium partition constant calculated as the ratio between the adsorption capacity ( $q_e$ ) and the equilibrium concentration ( $C_e$ ),  $R$  is the gas constant (8.314 J mol<sup>-1</sup> K<sup>-1</sup>), and  $T$  is the temperature in Kelvin (K).

From Eq. (8), a plot of  $\log K_d$  versus  $1/T$  (Fig. 8) reveals the  $\Delta H^0$  and  $\Delta S^0$  values. As shown in Tab. 4, the negative  $\Delta G^0$  value reveals that the process of tartrazine adsorption onto mixed-waste AC is spontaneous. A typical  $\Delta G^0$  value between 0 and -20 kJ mol<sup>-1</sup> indicates a physical adsorption process, whereas a more negative  $\Delta G^0$  value between -80 and -400 kJ mol<sup>-1</sup> indicates a chemical adsorption process [50–54]. In

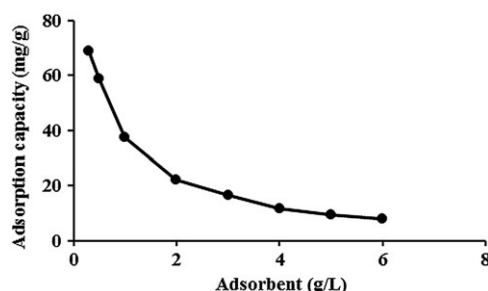


**Figure 7.** The effect of adsorbent concentration on tartrazine adsorption onto mixed-waste AC.

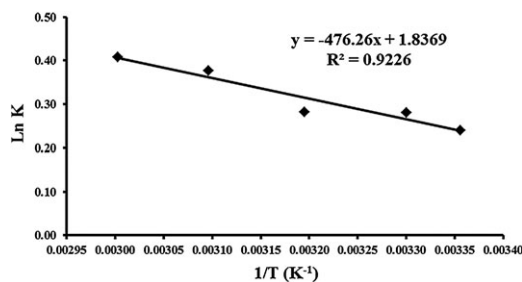


**Figure 8.** Thermodynamic study of the adsorption of tartrazine onto mixed-waste AC.

**Table 4.** Thermodynamic parameters for the adsorption of tartrazine onto mixed-waste AC

T (K)	Thermodynamic parameters		
	$\Delta G^0$ (kJ mol <sup>-1</sup> )	$\Delta S^0$ (J mol <sup>-1</sup> K <sup>-1</sup> )	$\Delta H^0$ (kJ mol <sup>-1</sup> )
298	-1.3	35.5	9.12
303	-1.6		
313	-1.7		
323	-2.3		

the present study, the values of  $\Delta G^0$  (-1.3 to -2.3 kJ mol<sup>-1</sup>) indicate a typical physical process. The values of  $\Delta H^0$  and  $\Delta S^0$  were obtained from the van't Hoff equation in the temperature range from 25 to 50°C as 9.12 kJ mol<sup>-1</sup> and 35.5 J mol<sup>-1</sup> K<sup>-1</sup>, respectively, at a pH 2 and using an initial tartrazine concentration of 100 ppm. The positive value of  $\Delta H^0$  (9.12 kJ mol<sup>-1</sup>) suggests that the adsorption process was endothermic, and the positive value of  $\Delta S^0$  (35.5 J mol<sup>-1</sup> K<sup>-1</sup>) indicates that the degree of freedom (or disorder) was increased.

## 4 Concluding remarks

Mixed-waste AC prepared by the simultaneous coprolysis of mixed solid waste (palm stems, paper, and plastic) by chemical and physical activation showed a high efficiency for the removal of tartrazine dye from aqueous solutions. The yield and carbon content of the mixed-waste AC increased as the calcium hydroxide concentration increased from 0.0 to 2 mol L<sup>-1</sup>. The maximum adsorption capacity for tartrazine removal was obtained at pH 2, a contact time of 300 min and an initial adsorbate concentration of 150 ppm. The kinetics of tartrazine adsorption followed the pseudo-second order rate model. The adsorption capacity of tartrazine at equilibrium increased from 19 to 74.9 mg g<sup>-1</sup> as the initial tartrazine concentration increased from 25 to 150 ppm. The thermodynamic parameters,  $\Delta G^0$ ,  $\Delta H^0$ , and  $\Delta S^0$ , showed that the adsorption was spontaneous and endothermic in nature.

## Acknowledgment

This work was supported by NPST program by King Saud University project number 09-ENV656-02.

The authors have declared no conflict of interest.

## References

- [1] D. Bilba, D. Suteu, T. Malutan, Removal of Reactive Dye Brilliant Red HE-3B from Aqueous Solutions by Hydrolyzed Polyacrylonitrile Fibres: Equilibrium and Kinetics Modeling, *Cent. Eur. J. Chem.* **2008**, *6*, 258–266.
- [2] P. P. Selvam, S. Preethi, P. Basakaralingam, N. Thinakaran, A. Sivasamy, S. Sivanesan, Removal of Rhodamine B from Aqueous Solution by Adsorption onto Sodium Montmorillonite, *J. Hazard. Mater.* **2008**, *155*, 39–44.
- [3] M. Wawrzkiwicz, Z. Hubicki, Use of Weakly and Strongly Basic Anion-Exchange Resins for the Removal of Indigo Carmine from Aqueous Solutions, *Przem. Chem.* **2008**, *87*, 711–714.
- [4] S. T. Ong, C. K. Lee, Z. Zainal, Removal of Basic and Reactive Dyes Using Ethylenediamine Modified Rice Hull, *Bioresour. Technol.* **2007**, *98*, 2792–2799.
- [5] J. H. Sun, S. P. Sun, G. L. Wang, L. P. Qiao, Degradation of Azo Dye Amido Black 10B in Aqueous Solutions by Fenton Oxidation Process, *Dyes Pigm.* **2007**, *74*, 647–652.
- [6] N. Dizge, C. Aydinler, E. Demirbas, M. Kobya, S. Kara, Adsorption of Reactive Dyes from Aqueous Solutions by Fly Ash: Kinetic and Equilibrium Studies, *J. Hazard. Mater.* **2008**, *150*, 737–746.
- [7] S. Aber, N. Daneshvar, S. M. Soroureddin, A. Chabok, K. Asadpour-Zeynali, Study of Acid Orange 7 Removal from Aqueous Solutions by Powdered Activated Carbon and Modeling of Experimental Results by Artificial Neural Network, *Desalination* **2007**, *211*, 87–95.
- [8] R. Gong, X. Zhang, H. Liu, Y. Sun, B. Liu, Uptake of Cationic Dyes from Aqueous Solution by Biosorption onto Granular Kohlrabi Peel, *Bioresour. Technol.* **2007**, *98*, 1319–1323.
- [9] A. Mittal, L. Kurup, J. Mittal, Freundlich and Langmuir Adsorption Isotherms and Kinetics for the Removal of Tartrazine from Aqueous Solutions Using Hen Feathers, *J. Hazard. Mater.* **2007**, *146*, 243–248.
- [10] T. Robinson, G. McMullan, R. Marchant, P. Nigam, Remediation of Dyes in Textile Effluent: A Critical Review on Current Treatment Technologies with a Proposed Alternative, *Bioresour. Technol.* **2001**, *77*, 247–255.
- [11] E. Forgacs, T. Cserhati, G. Oros, Removal of Synthetic Dyes from Wastewaters: A Review, *Environ. Int.* **2004**, *30*, 953–971.
- [12] A. A. Shabaka, S. G. Saad, M. S. Hassouna, M. G. Mohamed, M. M. Bereka, The Biodegradation of Some Cotton Textile Dyes, High Institute of Public Health, Alexandria University, Alexandria **2011**.
- [13] V. K. Gupta, A. Mittal, L. Krishnan, V. Gajbe, Adsorption Kinetics and Column Operations for the Removal and Recovery of Malachite Green from Wastewater Using Bottom Ash, *Sep. Purif. Technol.* **2004**, *40*, 87–96.
- [14] A. Mittal, L. Krishnan, V. K. Gupta, Use of Waste Materials – Bottom Ash and De-Oiled Soya, as Potential Adsorbents for the Removal of Amaranth from Aqueous Solutions, *J. Hazard. Mater.* **2005**, *117*, 171–178.
- [15] R. Gong, Y. Ding, M. Li, C. Yang, H. Liu, Y. Sun, Utilization of Powdered Peanut Hull as Biosorbent for Removal of Anionic Dyes from Aqueous Solution, *Dyes Pigm.* **2005**, *64*, 187–192.
- [16] T. Robinson, B. Chandran, P. Nigam, Effect of Pretreatment of Three Waste Residues, Wheat Straw, Corncocks and Barley Husks on Dye Adsorption, *Bioresour. Technol.* **2002**, *85*, 119–124.
- [17] R. Sanghi, B. Bhattacharya, Review on Decolorisation of Aqueous Dye Solutions by Low Cost Adsorbents, *Color. Technol.* **2002**, *118*, 256–269.
- [18] S. Saravanabhavan, K. J. Sreeram, J. Raghava Rao, B. Unni Nair, The Use of Toxic Solid Waste for the Adsorption of Dyes from Waste Streams, *J. Chem. Technol. Biotechnol.* **2007**, *82*, 407–413.
- [19] B. Ramaraju, P. Manoj Kumar Reddy, C. Subrahmanyam, Low Cost Adsorbents from Agricultural Waste for Removal of Dyes, *Environ. Prog. Sust. Energy* **2013**, published online. DOI: 10.1002/ep.11742
- [20] A. Gurses, S. Karaca, C. Dogar, R. Bayrak, A. Acikyildiz, M. Yalcin, Determination of Adsorptive Properties of Clay/Water System: Methylene Blue Sorption, *J. Colloid Interface Sci.* **2004**, *269*, 310–314.
- [21] T. C. Chandra, M. M. Mirna, Y. Sudaryanto, S. Ismajdi, Adsorption of Basic Dye onto Activated Carbon Prepared by Durian Shell: Studies of Adsorption Equilibrium Kinetic, *Chem. Eng. J.* **2007**, *127*, 121–129.
- [22] B. H. Hameed, F. B. M. Daud, Adsorption Studies of Basic Dye on Activated Carbon Derived from Agricultural Waste: *Hevea brasiliensis* Seed Coat, *Chem. Eng. J.* **2008**, *139*, 48–55.
- [23] B. H. Hameed, D. K. Mahmoud, A. L. Ahmad, Sorption Equilibrium and Kinetics of Basic Dye from Aqueous Solution Using Banana Stalk Waste, *J. Hazard. Mater.* **2008**, *158*, 499–506.
- [24] A. Debrassi, C. A. Rodrigues, Adsorption of Cationic Dyes from Aqueous Solution by Termite Feces, a Non-Conventional Adsorbent, *Clean – Soil Air Water* **2011**, *39*, 549–556.
- [25] X. S. Wang, J. P. Chen, Removal of the Azo Dye Congo Red from Aqueous Solutions by the Marine Alga *Porphyra yezoensis* Ueda, *Clean – Soil Air Water* **2009**, *37*, 793–798.
- [26] T. K. Saha, N. C. Bhoumik, S. Karmaker, M. G. Ahmed, H. Ichikawa, Y. Fukumori, Adsorption Characteristics of Reactive Black 5 from Aqueous Solution onto Chitosan, *Clean – Soil Air Water* **2011**, *39*, 984–993.

- [27] W. S. Wan Ngah N. F. M. Ariff, A. Hashim, M. A. K. M. Hanafiah, Malachite Green Adsorption onto Chitosan Coated Bentonite Beads: Isotherms, Kinetics and Mechanism, *Clean – Soil Air Water* **2010**, 38, 394–400.
- [28] Z. Yao, L. Wang, J. Qi, Biosorption of Methylene Blue from Aqueous Solution Using a Bioenergy Forest Waste: *Xanthoceras sorbifolia* Seed Coat, *Clean – Soil Air Water* **2009**, 37, 642–648.
- [29] K. V. Kumar, A. Kumaran, Removal of Methylene Blue by Mango Seed Kernel Powder, *Biochem. Eng. J.* **2005**, 27, 83–93.
- [30] I. Gaballah, D. Goy, E. Allain, G. Kilbertus, J. Thauront, Recovery of Copper through Decontamination of Synthetic Solutions Using Modified Barks, *Met. Metall. Trans.* **1997**, B28, 13–23.
- [31] T. Calvete, E. C. Lima, N. F. Cardoso, S. L. P. Dias, E. S. Ribeiro, Removal of Brilliant Green Dye from Aqueous Solutions Using Home Made Activated Carbons, *Clean – Soil Air Water* **2010**, 38, 521–532.
- [32] J. Zhu, H. Liang, J. Fang, J. Zhu, B. Shi, Characterization of Chlorinated Tire-Derived Mesoporous Activated Carbon for Adsorptive Removal of Toluene, *Clean – Soil Air Water* **2011**, 39, 557–565.
- [33] C. C. Chien, Y. P. Huang, W. C. Wang, J. H. Chao, Y. Y. Wei, Efficiency of Moso Bamboo Charcoal and Activated Carbon for Adsorbing Radioactive Iodine, *Clean – Soil Air Water* **2011**, 39, 103–108.
- [34] X. Yuan, X. Shi, S. Zeng, Y. Wei, Activated Carbons Prepared from Biogas Residue: Characterization and Methylene Blue Adsorption Capacity, *J. Chem. Technol. Biotechnol.* **2011**, 86, 361–366.
- [35] O. S. Bello, T. T. Siang, M. A. Ahmad, Adsorption of Remazol Brilliant Violet-5R Reactive Dye from Aqueous Solution by Cocoa Pod Husk-Based Activated Carbon: Kinetic, Equilibrium and Thermodynamic Studies, *Asia-Pacific J. Chem. Eng.* **2012**, 7, 378–388.
- [36] T. Santhi, S. Manonmani, Malachite Green Removal from Aqueous Solution by the Peel of *Cucumis sativa* Fruit, *Clean – Soil Air Water* **2011**, 39 (2), 162–170.
- [37] Y. Chen, W. Jiang, L. Jiang, X. Ji, Treatment of Dyeing Wastewater by Activated Carbons Derived from Municipal Sewage Sludge, *Environ. Prog. Sust. Energy* **2012**, 31, 585–590.
- [38] T. Senthilkumar, R. Raghuraman, L. R. Miranda, Parameter Optimization of Activated Carbon Production from *Agave sisalana* and *Punica granatum* Peel: Adsorbents for C.I. Reactive Orange 4 Removal from Aqueous Solution, *Clean – Soil Air Water* **2013**, 41 (8), 797–807.
- [39] R. S. Al-Jurf, F. A. Ahmed, I. A. Alam, H. H. Abdel-Rahman, Development of Heat Insulating Materials Using Date Palm Leaves, *J. Therm. Insul.* **1988**, 11, 158–164.
- [40] F. Pinto, C. Franco, R. N. André, C. Tavares, M. Dias, I. Gulyurtlu, I. Cabrita, Effect of Experimental Conditions on Co-Gasification of Coal, Biomass and Plastics Wastes with Air/Steam Mixtures in a Fluidized Bed System, *Fuel* **2003**, 82 (15–17), 1967–1976.
- [41] T. Chmielniak, M. Sciazko, Co-Gasification of Biomass and Coal for Methanol Synthesis, *Appl. Energy* **2003**, 74 (3–4), 393–403.
- [42] G. Collot, Y. Zhuo, D. R. Dugwell, R. Kandiyoti, Co-Pyrolysis and Co-Gasification of Coal and Biomass in Bench-Scale Fixed-Bed and Fluidized Bed Reactors, *Fuel* **1999**, 78 (6), 667–679.
- [43] R. Sivara, V. Rajendran, G. S. Gunalan, Preparation and Characterization of Activated Carbons from Parthenium Biomass by Physical and Chemical Activation Techniques, *Ej. Chem.* **2010**, 7 (4), 1314–1319.
- [44] C. Kütahyalı, M. Eral, Selective Adsorption of Uranium from Aqueous Solutions Using Activated Carbon Prepared from Charcoal by Chemical Activation, *J. Sep. Purif. Technol.* **2004**, 40, 109–114.
- [45] N. Sakayawong, P. Thiravetyan, W. Nakbanpote, Adsorption Mechanism of Synthetic Reactive Dye Wastewater by Chitosan, *J. Colloid Interface Sci.* **2005**, 286, 36–42.
- [46] P. Pengthamkeerati, T. Satapanajaru, O. Singchan, Sorption of Reactive Dye from Aqueous Solution on Biomass Fly Ash, *J. Hazard. Mater.* **2008**, 153, 1149–1156.
- [47] V. K. Singh, P. N. Tiwari, Removal and Recovery of Chromium(VI) from Industrial Waste Water, *J. Chem. Technol. Biotechnol.* **1997**, 69, 376–382.
- [48] Y. S. Ho, G. McKay, D. A. J. Wase, C. F. Foster, Study of the Sorption of Divalent Metal Ions on to Peat, *Adsorpt. Sci. Technol.* **2000**, 18, 639–650.
- [49] S. K. Srivastava, R. Tyagi, N. Pant, Adsorption of Heavy Metal Ions on Carbonaceous Material Developed from the Waste Slurry Generated in Local Fertilizer Plants, *Water Res.* **1989**, 23, 1161–1165.
- [50] M. Horsfall, A. I. Spiff, A. A. Abia, Studies on the Influence of Mercaptoacetic Acid (MAA) Modification of Cassava (*Manihot sculenta* Cranz) Waste Biomass on the Adsorption of  $\text{Cu}^{2+}$  and  $\text{Cd}^{2+}$  from Aqueous Solution, *Bull. Korean Chem. Soc.* **2004**, 25, 969–976.
- [51] Z. A. AlOthman, A. Hashem, M. A. Habila, Kinetic, Equilibrium and Thermodynamic Studies of Cadmium(II) Adsorption by Modified Agricultural Wastes, *Molecules* **2011**, 16, 10443–10456.
- [52] J. M. Smith, H. C. N. Van, *Introduction to Chemical Engineering Thermodynamics*, 4th Ed., McGraw-Hill, Singapore **1987**.
- [53] E. Malkoc, Y. Nuhoglu, Determination of Kinetic and Equilibrium Parameters of the Batch Adsorption Cr(IV) onto Waste Acorn of *Quercus ithaburensis*, *Chem. Eng. Process.* **2007**, 46, 1020–1029.
- [54] D. Sigh, Studies of the Adsorption Thermodynamics of Oxamyl on Fly Ash, *Adsorpt. Sci. Technol.* **2000**, 18, 741–748.